Mechanical and Spectroscopic Analysis of Retrieved/Failed Dental Implants

Umer Daood [1,*], Ninette Banday [2], Zohaib Akram [3] iD, James K. H. Tsoi [4] iD,
Prasanna Neelakantan [4], Hanan Omar [1], Tariq Abduljabbar [5], Fahim Vohra [5] iD,
Nawwaf Al-Hamoudi [6] and Amr S. Fawzy [7,8]

[1] Faculty of Dentistry, International Medical University, Wilayah Persekutuan Kuala Lumpur 57000, Malaysia;
     hanan_omar@imu.edu.my
[2] UAE Health Authority, Abu Dhabi 45728, United Arab Emirates; nbanday@dentexp.com
[3] Department of Periodontology, Faculty of Dentistry, Ziauddin University, Karachi 75600, Pakistan;
     drzohaibakram@gmail.com
[4] Faculty of Dentistry, The University of Hong Kong, Hong Kong; jkhtsoi@hku.hk (J.K.H.T.);
     prasanna@hku.hk (P.N.)
[5] Department of Prosthetic Dental Science, Faculty of Dentistry, King Saud University, Riyadh 60169,
     Saudi Arabia; academicksa1@gmail.com (T.A.); fahimvohra@yahoo.com (F.V.)
[6] Department of Periodontics and Community Dentistry, King Saud University, Riyadh 60169, Saudi Arabia;
     alhamoudink@gmail.com
[7] Faculty of Dentistry, National University of Singapore, Singapore 119083, Singapore; denasfmf@nus.edu.sg
[8] Oral Restorative and Rehabilitative Sciences, The University of Western Australia, Crawley,
     WA 6009, Australia
*   Correspondence: umerdaood@imu.edu.my; Tel.: +60-1-7309-4703

Abstract: The purpose of this study was to examine surface alterations and bone formation on the surface of failed dental implants (Straumann [ST] and TiUnite [TiUn]) removed due to any biological reason. In addition, failure analysis was performed to test mechanical properties. Dental implants ($n = 38$) from two manufacturers were collected and subjected to chemical cleaning. The presence of newly formed hydroxyapatite bone around failed implants was evaluated using micro-Raman spectroscopy. Scanning electron microscopy was used to identify surface defects. Mechanical testing was performed using a Minneapolis servo-hydraulic system (MTS) along with indentation using a universal testing machine and average values were recorded. A statistical analysis of mechanical properties was done using an unpaired t test, and correlation between observed defects was evaluated using Chi-square ($p = 0.05$). Apatite-formation was evident in both implants, but was found qualitatively more in the ST group. No significant difference was found in indentation between the two groups ($p > 0.05$). The percentage of "no defects" was significantly lower in the ST group (71%). Crack-like and full-crack defects were observed in 49% and 39% of TiUn. The ST group showed 11,061 cycles to failure as compared with 10,021 cycles in the TiUnite group. Implant failure mechanisms are complex with a combination of mechanical and biological reasons and these factors are variable with different implant systems.

Keywords: titanium; Raman; hydroxyapatite; failed; dental implant; mechanical; nanoindentation

1. Introduction

During the early development of dental implants, and since, many edentulous patients have benefitted from treatments that have increased options for teeth replacement. Treatment using dental implants for partially dentate patients is considered a feasible option, making occlusal

reconstruction possible for all types of patients [1]. Like any other restoration, dental implants also experience mechanical or biological complications [2]. These complications can be rectified within the implant prosthesis and, therefore, may not end up in failure. Some studies have reported technical complications within implant dentistry that have been the main reason for failures as mentioned above [2]. Dental implant loss can be categorized as "early" or "late" depending on the extent of the time period taken for that loss after implantation. Late losses of dental implants are considered when the prosthesis has failed after a period of six months [3].

In order to minimize failures, it is pivotal to understand the risk factors associated with failures and causing clinical complications. The primary predictors are chronic periodontitis, systemic diseases, poor quality of bone, smoking, and advanced age [4,5]. An all-important reason for loss of dental implants is mechanical complication. This may be due to mechanical damage to the implant itself, or to the supra-structure and mechanical supports. This leads to implant fractures, and can induce a severe complication of implant extraction with bone from the implanted area [6]. The defects and the design of an implant are highly unlikely reasons for an immediate or even late fracture. There are load factors, which directly correspond to the direction of occlusal forces applied. These fractures are primarily featured in molar and premolar regions of the mouth. Habits such as bruxism may result in an excessive overload on the implant system, making it one of the most common failures [7]. Implants with a smaller diameter are more vulnerable to fracture as compared with ones with larger diameters, in the posterior region [8]; it is important to keep in mind, however, that each dental implant used may have a mechanical history of its own as compared with implants lost as a result of controlled fatigue [9]. In addition, surface roughening procedures—which are particularly aimed at increasing osseointegration—may also contribute as a damaging factor. Surface changes such as scratches, dents, and craters may infest as additional causes for crack initiation and propagation [10].

There have been advances reported in implant dentistry, with the success criteria staying scarcely centered on patients. Like any other restoration, there is a probable chance that all will undergo a reduction in strength over a period of time [11]. Most implants do cross the expected longevity, after 10 years of service [12]. Hence, characterization of the mechanical problems remains a very important and huge task. The analysis presents an opportunity for diagnosis of the failure and failure pattern, which may be suitable to know for design improvements.

Proper use of analytical techniques is imperative to understanding the clinical performance of medical devices. Despite considerable advancement in ex-vivo techniques, these measures are seldom deployed to characterize chemical composition of the implant surface. Since the structure of bone crystals determines the ultimate strength, it is therefore essential to determine the chemical information of inorganic minerals to fully understand and explain the performance of an implant [13,14]. Raman spectroscopy has been used as a potential technique for studying bone quality and surfaces. The technique can provide non-destructive qualitative and quantitative analysis of organic and inorganic constituents of bone via characteristic vibrational frequencies [15]. It is a suitable technique to obtain information about the nature of calcium phosphate mineral phases, including hydroxyapatite [16].

Currently, there is minimal evidence on structural alterations and changes in the mechanical properties of implants [17]. The mechanical complications are common, showing a cumulative incidence of 1.8% in a follow-up done for up to 10 years [18]. Comprehensive analyses of retrieved dental implants are rare in biomechanical and dental literature, as incidences of fractures and failures are considered low. Scanning electron microscopy revealed intra-oral fractures and fatigue striations in dental implants [19]. However, studies did not show any failure analysis of retrieved implants under lab conditions which can provide some information on the operating mechanisms of dental implants. Most of the literature available does not comment on stress against the number of cycles to failure analysis [20]. Hence, the aim of this study was to examine the surface of failed dental implants that were removed due to any biological reason. The hypothesis was that retrieved or failed dental implants have surface and mechanical property alterations after use. In addition, the surface

properties of retrieved dental implants were analyzed by Raman spectroscopy to determine bone (apatite) formation around the implant surface. The metal composition of the implants was also checked. The analysis was also performed in SEM-EDX (energy dispersive X-ray spectroscopy in the scanning electron microscope). This identification is semi-quantitative, but allows the establishment of a clear distinction between the implants. The above studies illustrate the partial information on the retrieved dental implants. One can predict that there may be increased incidence of mechanical failures and complications with the passage of time. Therefore, exemplar testing was also performed complimented with nanoindentation testing to predict structural alterations and changes in mechanical properties after failure.

2. Materials and Methods

2.1. Implant Specimens

Thirty-eight dental implants were retrieved from 43 patients (mean age [±SD] considered was 50 ± 13.2 years) who underwent implant surgery (in Saudi hospital/OPD, Riyadh, Saudi Arabia) during a period of 6 years. The patients' informed consent was obtained under a protocol approved by the Institutional and Ethical Review Board of King Saud University (FR-2017-46), explaining to them the use of the retrieved implants for scientific research. All efforts were made to protect the complete anonymity of the patient. The implants were collected from the upper and lower jaw, with failure most likely due to lack of bone support (suggested by operators). In addition, the retrieved implants were investigated for solely technical reasons, without addressing any medical issues. Although the patients' medical background information was known, the information was not really considered. All implants that have failed within 6 years of their placement (2010–2016) were included. The study population included 23 males and 20 females. Failures were detected by measuring peri-implant radiographic examination, bleeding on probing, suppuration, and mobility. As soon as the implants were retrieved, specimens were stored in brand-new sterile plastic bottles. This procedure was monitored and carefully handled to avoid excessive and subsequent contamination. Dental implants studied were of a cylindrical design, with an implant diameter of 3.6 mm and lengths of 8 to 10 mm. These measurements were not part of the inclusion criteria. Previously, implant placements were carried out according to the following indications: single-tooth, partial edentulism (two or more implants), and complete edentulism under local anesthesia using the Swedish protocol [21]. Twenty Straumann dental implants (Institute Straumann, Waldenburg, Switzerland) were retrieved after 6 years, while one was immediately retrieved after increased mobility (less than 6 years implant failure). Seventeen other dental implants were also retrieved (TiUnite®, Nobel Biocare, Goteborg, Sweden) and analyzed by the same protocol described previously.

Surface Cleaning of Dental Implants

The cleaning protocol for all retrieved implants and implant parts involved the use of chemical solutions for the removal of blood/soft tissue along with organic layers. The retrieved specimens were inserted into 100 mL glass beakers filled with different chemical solutions for removal of debris. The specimens were completely inserted inside. Three percent sodium hypochlorite solution was used for the removal of blood/soft tissue in < 10 min. Pure acetone (CAS 67-41-1; Sigma Aldrich, St. Louis, MI, USA) was used for 30 min to remove organic layers. There was no effort to remove the inorganic layer; this was to carry out the analysis of hydroxyapatite bone crystals. While the specimens were inside the solution, the beaker was kept on a hot water ultrasonic bath. Specimens were thoroughly rinsed with water or ethyl alcohol between placement in different solutions.

2.2. Backscattering Scanning Electron Microscopy Analysis of Failed Implant Surfaces

Retrieved failed dental implants (*n = 9* for each group; ST & TiUn) and control specimens were visualized using SEM in a back-scattering mode. Samples were rinsed with PBS and post-fixed for

1 h using (1%) osmium tetraoxide. After rinsing with PBS again, the specimens were subjected twice to dehydration in an ascending series of ethanol solutions (75%, 85%, 95%, and 100%, 60 min each). Specimens were then mounted with conductive tape on aluminum stubs (double-sided carbon tape) in such a way that they could be observed in a cross-sectional view and later stored in a desiccator for 24 h. They were sputter coated with a 30 nm thick (pre-set) layer of gold palladium alloy for 120 s and viewed at different magnifications using SEM (Hitachi S-3400N, Hitachi High Technologies America, Inc., Schaumburg, IL, USA) operated at an accelerating voltage of 10 kV. The images viewed on the monitor were evaluated by two examiners. The implants were specifically examined for early signs of mechanical failure (cracks) through a surface scanning of the entire periphery of the implant surface (360°). While examining, a few considerations, like identification of any surface treatment and location of defects, were taken into account. The dental implant samples (two implants each for both systems) were also analyzed by EDS (Joel, JSM-6380A Analytical Scanning Electron Microscope with EDS elemental analyzer, Tokyo, Japan) to verify the compositions of the materials by taking an electron beam voltage of 15 kV and a beam current less than 3×10^{-7}.

2.3. Raman Spectroscopy Measurements

Raman spectroscopy was used to analyze the chemical composition and crystallinity of bone crystals present on failed dental implant surfaces (ST & TiUn). With this spectroscopic approach, the molecular properties of the newly formed bone around the failed implant (*n = 4* for each group; ST & TiUn) could be evaluated. Micro-Raman measurements were performed using a Jasco NRS-2000C instrument (Jasco Inc., Easton, MD, USA). The spectrometer was connected to a microscope with $100\times$ magnification and a 160 K frozen CD detector (Spec-10: 100B, Roper Scientific Inc., Trenton, NJ, USA). Spectral recording was done in a back-scattering mode (1 cm^{-1} spectral resolution) using a $100\times$ objective lens, with an argon ion 514.5 nm laser at 785 nm wavelength (spectral resolution of 1.6 cm^{-1}), and power < 500 µW with a superior signal/noise ratio having a laser driver power of about 5 mW. This was essential to allow a focus of 1 µm diameter within the sampling area. The spectrometer was set to operate in a confocal mode, with a slit opening of 11 µm, and a grating of 1200 mm^{-1}. In the confocal mode, a spatial resolution of a 1–2 µm within the *x–y* plane was achieved. The spectra were recorded covering a total frequency range of 400–1800 cm^{-1}. Characteristic Raman signatures were then selected as peaks, limited by a linear background. In order to obtain a descent representation of the specimens, six frames of 30 s exposure were recorded and later subjected to system background removal, spectral analysis, and dark count correction. The intensities were completely normalized for final analysis. All spectra were recalibrated to the amplitude of the respective spectra. These spectra were presumed to have contributed from the implant surface normalized around the 960 cm^{-1} region. No sample degradation is expected upon laser irradiation as Raman spectroscopy causes minimal changes on the specimens.

2.4. Fatigue Testing

The cyclic mechanical testing was carried out using a Minneapolis servo-hydraulic system (MTS, Minneapolis, MN, USA, with a 250 kN load capacity [22]. The machine was driven under load control. In order to fix the testing implants on the machine, a custom-designed steel cage holding was machined containing a slotted steel cylinder. The implants were tested (*n = 3* for each group having same batch number with bone residues on the surface; ST & TiUn) under dry conditions and kept inside the steel cylinder up to the second thread around the head of the implant. The specimen holder was then inserted inside the holding stage at an angle of 30°, fixing it to the testing machine. This positioning converted the testing force into a bending moment applied to the implant abutment, according to the static bend strength of the retrieved implant specimens (ISO 14801 recommendation/standard for dynamic fatigue testing for dental implants) [23]. At a displacement rate of 0.4 mm/min, quasi-static bending strength (a vertical load) was applied until the retrieved implant underwent a permanent plastic deformation or fracture, followed by a load drop. The machine was stopped when 5×10^6 cycles

had acceded without apparent failure. The machine automatically stopped after fracture and recorded sinusoidal loads with minimum to maximum loading ratio of $R = 0.1$, with test frequencies in the range of 2–15 Hz (ISO 14801 recommendations). All cyclic loads for each retrieved implant were scaled or normalized to their quasi-static test strength in the range of 0–1. The specimens were rigidly clamped at the base, which appeared more severe as compared with in vivo flexible conditions experienced by a dental implant. However, these rigid clamping conditions did not seem to affect conclusions drawn from the results. The testing was performed under ambient room temperatures.

2.5. Instrumented Indentation Testing

Three specimens from each retrieved implant group (*n = 3*) were embedded in an epoxy resin (Epofix, Hatfield, PA, USA) along a longitudinal axis and were cut in the middle with a Struers diamond cut-off wheel (Struers, Denmark), ground with 2000 grit SiC papers, and polished with diamond pastes (DP, Struers) up to 1 μm in a grinding polishing machine (*Buehler* Minimet 1000 *Polisher*/Grinder, Lake Bluff, IL, USA). After cleaning the specimens inside an ultrasonic bath, the elastic index (η_{IT}; elastic to total work ratio) and indentation modulus (E_{IT}) were determined using a (instrumentation indentation) universal hardness testing machine (Zwick Roell, Ulm, Germany). Five indentation force depth curves were recorded for each specimen using a Vicker's indenter (CSM Instruments, Peseux, Switzerland) with a 9.8 N load for 10 sec contact time. The average values for mechanical testings were recorded to characterize the retrieved dental implant specimens.

2.6. Statistical Analysis

All mechanical properties were statistically compared by an unpaired t test at a 95% confidence interval. All data were checked for normality using Shapiro–Wilk tests. The correlation between the observed defects was evaluated using Chi-square tests with the significance level set to $p = 0.05$.

3. Results

3.1. SEM/EDX Interfacial Analysis

The mechanical defects of dental implant surfaces were identified via SEM (Figure 1). The SEM images of the ST control specimens (Figure 1A) and TiUn (Figure 1B) showed a homogenous titanium surface with some irregular striations as a result of the industrial machining process. Any lengths of crack formation seen amongst the implants between 25 μm and 100 μm were characterised as "crack-like defects" [24]. Out of the implants selected, 43% contained observed defects on examined implants. This is in contrast to 74% of the implants observed showing crack-like defects. There were no signs of surgical instrument marking nor any signs of wear. This was a strong indication that the present crack-like defects were generated during the use of the implant inside the patient's mouth. The SEM micrograph (Figure 1C,D) illustrated surface defects in the TiUn groups (39%). The defects were quite abundant and consisted essentially of superficial craters. "Crack-like" (49%) defects were also seen on the inserted implant TiUn surface (Figure 1E). These cracks appeared deeper as characteristic of full cracks and slightly wider. However, the SEM analysis in the apical portion of the ST implant surface showed no cracks and were less abundant overall (13%). Similarly, 27% of crack-like defects were observed amongst ST implants in the present work (Table 1).

The retrieved Straumann implant surface analysis (Figure 2) showed ingrowth and anchorage of bone on the implant surface depicting a fracture of bone rather than a complete coverage on top of the implant surface (Figure 2A). The SEM results show a fibrinous matrix with a less osseous surface (Figure 2B). A slightly higher degree of mineralization was observed in Straumann implants (Figure 3A), confirming the intimate contact of mature lamellar bone in the ST group. No foreign bodies were detected on the observed mentioned areas of bone. The ST group shown in the figure indicated the presence of Ca and Ti peaks. The presence of Ca indicated newly formed particles on the implant surface with trace quantities of sodium and chloride (data not shown).

High-magnification interfacial analysis revealed well-identified Ti and presented an irregular and ill-defined interface between implant and bone (Figure 3B) in the TiUn group. TiUn had a progressively higher reduction from metal to bone with increased Ca and P than in the case of the Straumann dental implants.
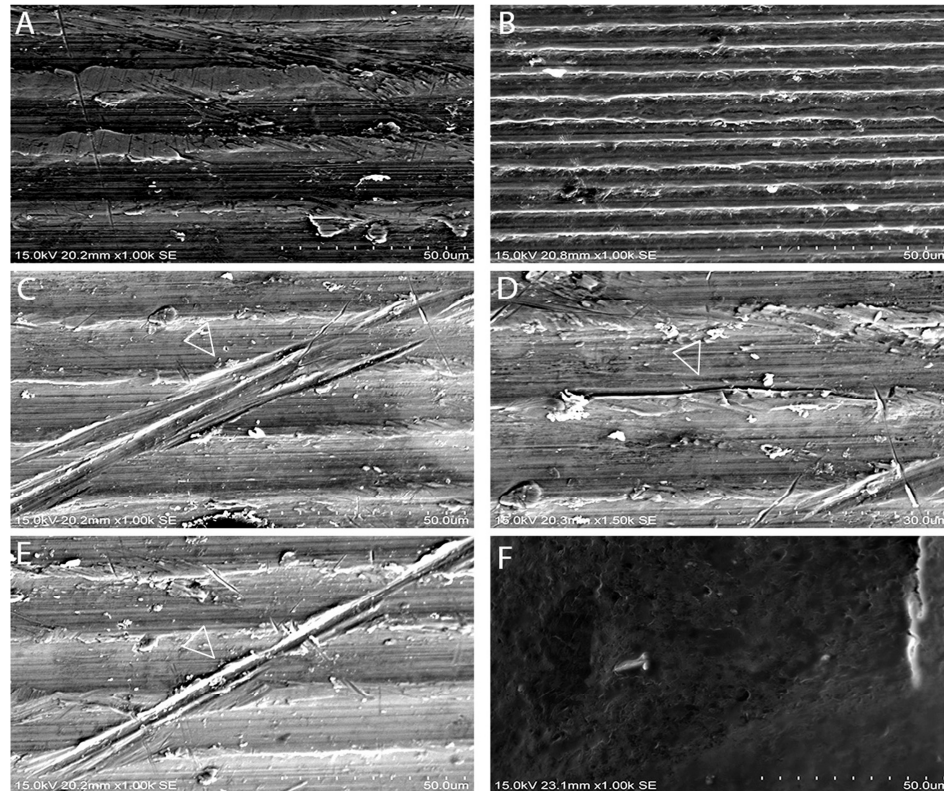
Figure 1. Surface analysis of retrieved dental implants. (**A**) Titanium Straumann (ST), Waldenburg, Switzerland implant control group (new); (**B**) TiUnite® (TiUn), Goteborg, Sweden; (**C**,**D**) SEM micrographs of surface defects in TiUn retrieved implants (white arrow). The defects were quite abundant and consisted essentially of superficial craters; (**E**) SEM micrographs of surface defects defined as "crack-like" in TiUn (white arrow). These cracks appeared deeper as characteristic of full cracks and slightly wider; (**F**) SE analyses of the apical portion of titanium Straumann.
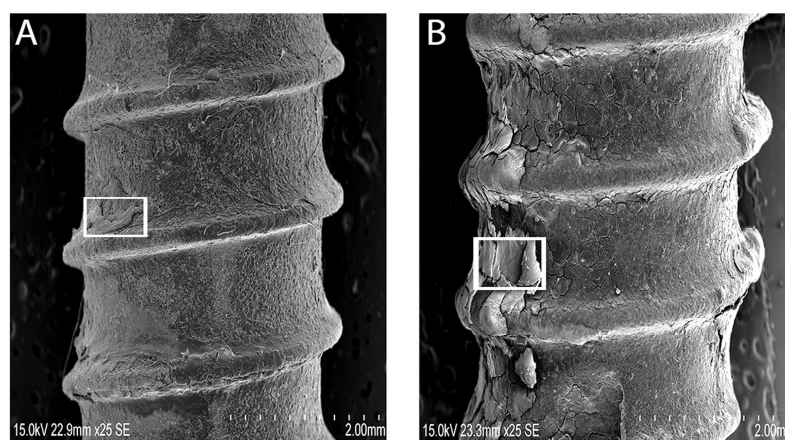
Figure 2. (**A**) SEM images from the surface of ST groups; (**B**) Presence of bone-like augments can be identified (white box) within the implant serrations. The boxed regions represent the area of Raman spectroscopy where part of hydroxyapatite bone formation was analyzed.
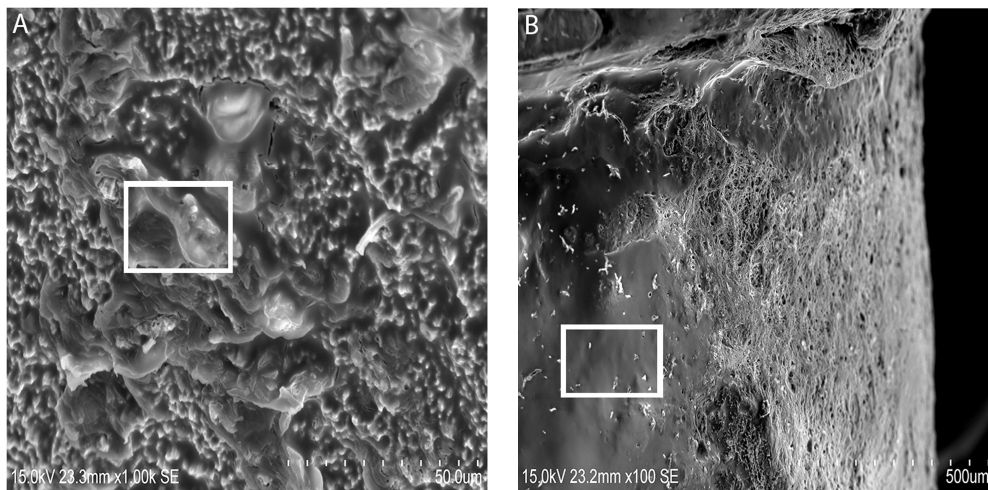
Figure 3. Representative SEM images from the surface of (**A**) ST group with random distribution of parts like bone formation at a higher magnification; Representative SEM images from the surface of (**B**) TiUn group with bone-like formations identified on their surface, confirmed with Raman analysis. (Boxed areas showing deposits later confirmed for apatite structure using Raman spectroscopy.)

**Table 1.** Observed defects on the implant surfaces.

Implant Type	Defects						p-Value
	No Defects		Crack-Like Defects		Full Cracks		
	N	%	N	%	N	%	
ST	4	75	2	0	3	33	$p = 0.003$
TiUn	4	25	2	50	3	67	$p = 0.004$

Note: Implant defects with total number of implants and the percentage of defects seen.

3.2. Raman Data Acquisition

Raman spectroscopy was employed to examine the molecular identity of apatite formation along the surfaces of as-received retrieved dental implants. Figure 4 shows the representative Raman spectra of failed dental implants/ST and TiUn groups demonstrating somewhat different spectral features. The peak at 960 cm^{-1} is primarily associated with the vibrational stretch of phosphate (PO_4^{3-}) (Figure 4A). The presence of these peaks within retrieved implants demonstrated that there was mineralization. However, the bone apatite changes were more pronounced in the ST groups as compared with the TiUn groups. This hypothesis was confirmed by the spectrum recorded at the laser power showing more broadening of peaks in the Straumann implants. Within the ST group, the Raman peaks at 960 cm^{-1} and 2940 cm^{-1} appeared pronounced. The peak at 2940 cm^{-1} appears to project the CH bonds representing the bone organic matrix (Figure 4B) showing the influence of collagen deposition. A higher peak showing more deposition of organic matrix will indicate a higher mineralization, as seen in the ST implant system. It was apparent that the PO_4^{3-} stretching region appeared the most sensitive region dominating the spectrum of the ST implant surfaces. The TiUn groups demonstrated ill-defined peaks of inorganic crystalline structure with just broad fills and rises within intensities.
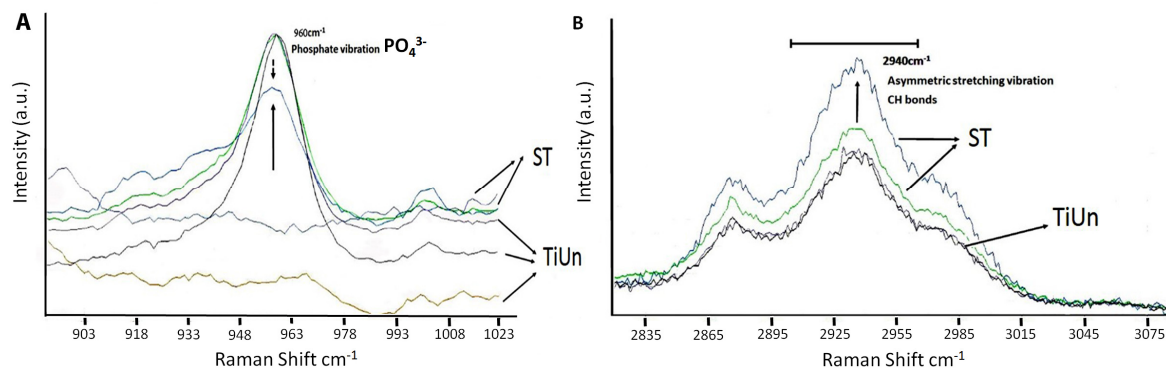
Figure 4. (**A**) Representative micro-Raman spectra recorded on the surface of received implants at a laser power of 5 mW showing marked differences within the intensities attributed to symmetric stretching vibration of PO_4^{3-} (inorganic phosphate); (**B**) Representative micro-Raman spectra recorded on the surface of the implants showing the main peak centered at 2940 cm^{-1} related to CH bonds.

3.3. Mechanical Properties (Fatigue Testing and Nanoindentation)

Table 2 represents the fatigue test results after cyclic loading to failure tested in lab conditions in room temperature. The results obtained showed the fractographic characterization of fatigued failed dental implants.

Table 2. Fatigue test results.

Groups	Load	No. of Cycles to Failure
Straumann	1125 N	11,061
TiUnite®	980 N	10,021

The representative force indentation depth curves from both groups appear in Figure 5. The results of the nano-indentation analysis are presented in Table 3. There was no significant difference found between the two groups.
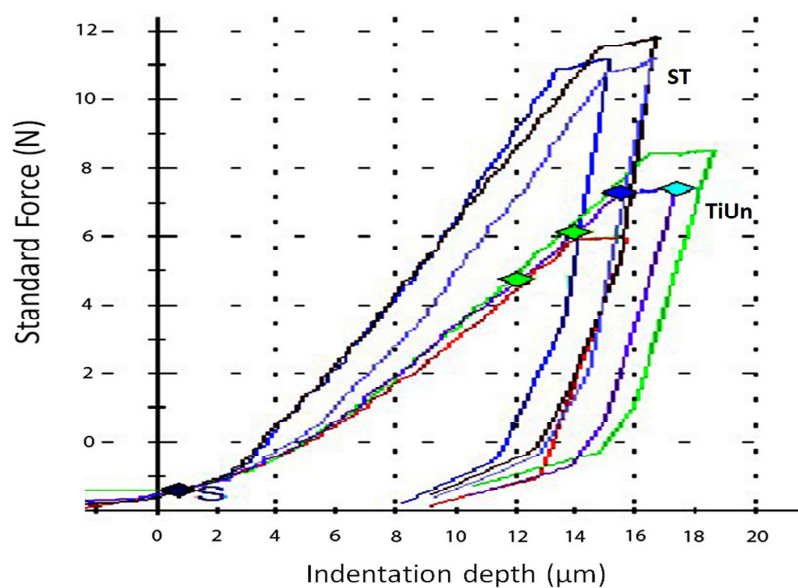
Figure 5. Representative load indentation depth curves for the ST and TiUn implants tested.

Table 3. Mean values and standard deviations of the mechanical properties tested. There were no statistical differences identified between the groups ($p > 0.05$). E_{IT}, indentation modulus; η_{IT}, Elastic index, failed implants.

Groups	E_{IT} (GPa)	Elastic Index η_{IT} (%)
Straumann	37 (4)	25 (1)
TiUnite®	34 (2)	23 (2)

4. Discussion

Despite the fact that the implants showed bone residues covering the implant surface, the dental implants may have failed due to progressive reduction of bone support or biological support. Yet, the qualitative analysis of bone on retrieved dental implants necessitated consideration of surface analysis for any mechanical crack formations. The retrieved implants were considered as "in-vivo" undergoing repeated loading inside the oral cavity, presenting enough evidence of oral stresses and its environment on mechanical integrity. Clinically failed dental implants were encapsulated with soft tissues, but showed areas of bone (Figure 2A,B). In addition, there were alterations in the mineral composition and accumulation of organic material with retained oral integuments and bone-like formations inside ST implants (Figure 2C). The elemental composition of retrieved ST implants with bone-like formations was dominated with Ca and Na. Both groups of implants revealed a bone-like covering (Figure 3A,B) with distinct gaps between the implant and bone. This may be due to the complex interaction of the implant surface with the biological environment into which it was inserted. Hydroxyapatite dissolution and reprecipitation can occur along the bone implant interface [25]. The presence of a phosphate peak at 960 cm^{-1} within the Raman spectrum supports the possibilities (Figure 4) related to the presence of bone formation. The SEM images showed deposition on the surface of ST implants, which the authors speculated as hydroxyapatite crystals (Figure 3A,B). This is in conjunction to the presence of a hydroxyapatite peak found in the Raman spectroscopy result. By comparing the SEM images (Figure 3A,B), one can observe the aspect of the new bone surface which seems more dense in ST implant groups (Figure 3A) as compared with TiUn (Figure 3B). The TiUn groups were associated with crack-like defects or full cracks with a statistical difference. The results (Table 1) indicate the proportion of defects found in both implant groups, further strengthening the fact that the TiUn implant groups had more reasons to fail. The surface of TiUn implants showed cracks in the vicinity of main cracks but showed no indication of a final fracture within the implant. Therefore, the hypothesis that retrieved or failed dental implants have surface property alterations can be partially rejected.

Surface characterizations of retrieved or failed dental implants have gained a lot of interest in the last years as a tool to interpret failure mechanisms [26]. In an effort to eradicate variability in results due to placement of different dental implants amongst patients, only two types of implants were included in this study. This study was based on a random selection of implants of two different companies having undergone different surface preparation and lengths. Therefore, the samples collected are considered as representatives of the types of implants used in clinical implant dentistry. This failure analysis is reflective of the causes and means to understand and prevent failure reoccurrence by improving the dental implant's biological and mechanical performance inside the oral cavity [27]. The exposure of dental implants to any liquid medium mimicking oral environmental conditions was avoided and tests were performed in dry-air laboratory conditions, as received.

Raman spectroscopy enabled qualitative analysis at a molecular level, where it can predict the presence of bone and its maturity. It is an optical tool for less invasive and less destructive analysis of biological samples, giving precise information on biochemical composition [28]. Many have accepted Raman spectroscopy as a viable tool for study of bone mineralization and analysis. The Raman spectra interfered with the fluorescence of biological specimens and hence is preferred over infra-red spectroscopy [29]. By chemical mapping and monitoring peak intensities at 960 cm^{-1} (PO_4^{3-}) and 2940 cm^{-1} (CH bonds), it was possible to distinguish which implant type had bone growth around

its surface. In the present study, the increased organic and inorganic peaks (Figure 4A,B) showed an osseo-integration somehow taking place. The increase in the quality and sharpness of Raman peaks at 960 cm^{-1} (chemical signature for bone) amongst ST implants was due to slightly more bone deposition on the implant surface, known as hydroxyapatite coverage. It is important to note that, despite being not statistically significant, the results of 960 cm^{-1} amongst the ST implants at the surface of the inserted sites showed the same level of bone deposition in all specimens. We found a difference in Raman spectroscopic intensities between the two groups as the ST groups showed higher peak intensities than the TiUnite groups (Figure 4A,B). The organic peaks at 2940 cm^{-1} related to the CH bonds were found, showing the influence of collagen deposition (Figure 4B). The organic bone matrices are primarily made up of type I collagen [30,31], synthesized by osteoblasts, that is mineralized with hydroxyapatite during the later stages of osteogenesis [32]. Therefore, the higher deposition seen amongst the ST groups indicated a higher mineralization. In the present study, this correlation was found between the organic (2940 cm^{-1}) and inorganic contents (960 cm^{-1}), in particular within the ST groups. The ST implant surface was almost completely covered with the layer of bone minerals, with the exception of one peak in the TiUn group that showed higher crystallinity comparable to the ST group. The crystallinity of the formed bone is known to influence the clinical performance of the bone implant. The crystalline bone is less susceptible to dissolution leading to rapid supersaturation phosphate and calcium ions in the implant environment [33]. When hydroxyapatite is low in crystallinity, this will elevate the local pH, resulting in a lesser cell proliferation and a lesser bone volume [34]. Therefore, the hypothesis that retrieved or failed dental implants have surface property alterations can be partially rejected.

In order to understand the failure analysis, the study partly comprised fatigue testing to identify the fatigue fracture mechanism amongst the two groups. The results (Table 2) indicate that the oral environment may have caused the significant reduction in the TiUn group. The authors speculate that the oral environment may have been a significant factor in the overall failure of the implants. The study did not identify or analyze corrosion mechanisms as this point was not elucidated in the project. This should be pivotal in future studies to analyze the fatigue or failure of dental implants. A typical biting force in an adult is close to 38.8 N to 661.5 N in upper first molars [35].

Indentation techniques have been widely used for assessing bone tissue micromechanical properties [36,37]. Based on the results of this study, the null hypothesis was accepted, as retrieved implants demonstrate morphological alterations but no statistical differences. The indentation modulus (E_{IT}) at the surface-to-core cross sections of both the implant systems is less than half that of titanium (103 GPa) [38]. It can be speculated that there could have been damage during implant insertion due to high profile of the bone. The presence of bone around the implant can be inferred by the elastic modulus measured by the indentation. The unexpectedly low Young's modulus of the surface maybe also be due to testing of the bone on the implant surface rather than the alloy. There were no statistical differences between the two groups as far as the elastic index was concerned.

Special considerations were taken not to remove any inorganic layers on the retrieved dental implants by the use of sodium hypochlorite solution at a concentration of 3%. After cleaning with the solution, thorough rinsing of the implants was performed using water or ethyl alcohol to make sure there was no contamination left behind. Future studies are required to analyze any contamination due to the cleaning protocol and comparison studies for surface defects before implantation.

5. Conclusions

The failure mechanisms of the ST implant group remain unclear, with biological failure and reduced bone apposition against the TiUn groups the likely cause. The crystalinity of the formed bone is known to influence the clinical performance of the bone implant. Implant failure mechanisms are complex with a combination of mechanical and biological reasons, and these factors are variable with different implants. The surface of TiUn implants showed cracks in the vicinity of main cracks but no indication of a final fracture within the implant.

Conflicts of Interest: The authors declare no conflict of interest.

References

1. Kobayashi, Y.; Sumida, T.; Ishikawa, A.; Mori, Y. The contribution of dental implants to functional artificial restoration after treatment of oral cancer. *Anticancer Res.* **2016**, *36*, 3053–3056. [PubMed]

2. Pjetursson, B.; Asgeirsson, A.; Zwahlen, M.; Sailer, I. Improvements in implant dentistry over the last decade: Comparison of survival and complication rates in older and newer publications. *Int. J. Oral Maxillofac. Implant.* **2014**, *29*, 308–324. [CrossRef] [PubMed]

3. Goodacre, C.J.; Bernal, G.; Rungcharassaeng, K.; Kan, J.Y. Clinical complications with implants and implant prostheses. *J. Prosthet. Dent.* **2003**, *90*, 121–132. [CrossRef]

4. Alsaadi, G.; Quirynen, M.; Michiles, K.; Teughels, W.; Komárek, A.; Van Steenberghe, D. Impact of local and systemic factors on the incidence of failures up to abutment connection with modified surface oral implants. *J. Clin. Periodontol.* **2008**, *35*, 51–57. [CrossRef] [PubMed]

5. Alsaadi, G.; Quirynen, M.; Komárek, A.; Van Steenberghe, D. Impact of local and systemic factors on the incidence of oral implant failures, up to abutment connection. *J. Clin. Periodontol.* **2007**, *34*, 610–617. [CrossRef] [PubMed]

6. Papaspyridakos, P.; Chen, C.J.; Chuang, S.K.; Weber, H.P.; Galluci, G.O. A systematic review of biologic and technical complications with fixed implant rehabilitations for edentutlous patients. *Int. J. Oral Maxillofac. Implant.* **2012**, *27*, 102–110.

7. Eckert, S.E.; Meraw, S.J.; Cal, E.; Ow, R.K. Analysis of incidence and associated factors with fractured implants: A retrospective study. *Int. J. Oral Maxillofac. Implant.* **2000**, *15*, 662–667.

8. Green, N.T.; Machtei, E.E.; Horwitz, J.; Peled, M. Fracture of dental implants: Literature review and report of a case. *Implant Dent.* **2002**, *11*, 137–143. [CrossRef]

9. Shemtov-Yona, K.; Rittel, D.; Levin, L.; Machtei, E.E. Effect of dental implant diameter on fatigue performance. Part I: Mechanical behavior. *Clin. Implant Dent. Relat. Res.* **2014**, *16*, 172–177. [PubMed]

10. Shemtov-Yona, K.; Rittel, D.; Dorogy, A. Mechanical assessment of grit blasting surface treatments of dental implants. *J. Mech. Behav. Biomed. Mater.* **2014**, *39*, 375–390. [CrossRef] [PubMed]

11. Papaspyridakos, P.; Chen, C.J.; Singh, M.; Weber, H.P.; Gallucci, G.O. Success criteria in implant dentistry: A systematic review. *J. Dent. Res.* **2012**, *91*, 242–248. [CrossRef] [PubMed]

12. Setzer, F.C.; Kim, S. Comparison of long-term survival of implants and endodontically treated teeth. *J. Dent. Res.* **2014**, *93*, 19–26. [CrossRef] [PubMed]

13. Landis, W.J. The strength of a calcified tissue depends in part on the molecular structure and organization of its constituent mineral crystals in their organic matrix. *Bone* **1995**, *16*, 533–544. [CrossRef]

14. Ghanem, A.; Abduljabbar, T.; Akram, Z.; Vohra, F.; Kellesarian, S.V.; Javed, F. A systematic review and meta-analysis of pre-clinical studies assessing the effect of nicotine on osseointegration. *Int. J. Oral Maxillofac. Surg.* **2017**, *46*, 496–502. [CrossRef] [PubMed]

15. De Souza, R.A.; Xavier, M.; Da Silva, F.F.; de Souza, M.T.; Tosato, M.G.; Martin, A.A.; de Melo Castilho, J.C.; Ribeiro, W.; Silveira, L. Influence of creatine supplementation on bone quality in the ovariectomized rat model: An FT-Raman spectroscopy study. *Lasers Med. Sci.* **2012**, *27*, 487–495. [CrossRef] [PubMed]

16. Sauer, G.R.; Zunic, W.B.; Durig, J.R.; Wuthier, R.E. Fourier-transform Raman-spectroscopy of synthetic and biological calcium phosphates. *Calcif. Tissue Int.* **1994**, *54*, 414–420. [CrossRef] [PubMed]

17. Eliades, T.; Zinelis, S.; Papadopoulos, M.A.; Eliades, G. Characterization of retrieved orthodontic miniscrew implants. *Am. J. Orthod. Dentofac. Orthop.* **2009**, *135*, 10.e1–10.e7. [CrossRef]

18. Pjetursson, B.A.; Tan, K.; Lang, N.P.; Brägger, U.; Egger, M.; Zwahlen, M. A systematic review of the survival and complication rates of fixed partial dentures (FPDs) after an observation period of at least 5 years. *Clin. Oral Implant. Res.* **2004**, *15*, 667–676. [CrossRef] [PubMed]

19. Sbordone, L.; Traini, T.; Caputi, S.; Scarano, A.; Bortolaia, C.; Piattelli, A. Scanning electron microscopy fractography analysis of fractured hollow implants. *J. Oral Implantol.* **2010**, *36*, 105–112. [CrossRef] [PubMed]

20. Hertzberg, R.W. Cyclic stress and strain fatigue. In *Deformation and Fracture Mechanics of Engineering Marerials-3*; John Wiley and Sons: Hoboken, NJ, USA, 1989; pp. 457–507.

21. Adell, R.; Lekholm, U.; Rockler, B.; Brånemark, P.I. A 15-year study of osseointegrated implants in the treatment of the edentulous jaw. *Int. J. Oral Surg.* **1981**, *10*, 387–416. [CrossRef]

22. Keren-Shemtov, Y.; Daniel, R. Identification of failure mechanisms in retrieved fractured dental implants. *Eng. Fail. Anal.* **2014**, *38*, 58–65. [CrossRef]

23. *ISO 14801 Fatigue Test for Endosseous Dental Implants*; International Organization for Standardization: Geneva, Switzerland, 2007.

24. Shemtov-Yona, K.; Rittel, D. On the mechanical integrity of retrieved dental implants. *J. Mech. Behav. Biomed. Mater.* **2015**, *49*, 290–299. [CrossRef] [PubMed]

25. Randorn, C.; Kanta, A.; Yaemsunthorn, K.; Rujijanakul, G. Fabrication of dense biocompatible hydroxyapatite ceramics with high hardness using a peroxide-based route: A potential process for scaling up. *Ceram. Int.* **2015**, *41*, 5594–5599. [CrossRef]

26. Azevedo, C.R.; Hippert, E. Failure analysis of surgical implants in Brazil. *Eng. Fail. Anal.* **2002**, *9*, 621–633. [CrossRef]

27. Shemtov-Yona, K.; Rittel, D.; Levin, L.; Machtei, E. The effect of oral-like environment on dental implants' fatigue performance. *Clin. Oral Implant. Res.* **2014**, *25*, e166–e170. [CrossRef] [PubMed]

28. Oliveira, A.P.; Bitar, R.A.; Silveira, L.; Zangaro, R.A.; Martin, A.A. Near-infrared Raman spectroscopy for oral carcinoma diagnosis. *Photomed. Laser Surg.* **2006**, *24*, 348–353. [CrossRef] [PubMed]

29. Morris, M.D.; Stewart, S.; Tarnowski, C.P.; Shea, D.; Franceschi, R.; Wang, D.; Ignelzi, M.A., Jr.; Wang, W.; Keller, E.T; Lin, D.L.; et al. Early mineralization of normal and pathologic calvaria as revealed by Raman spectroscopy. In Proceedings of the International Symposium on Biomedical Optics, San Jose, CA, USA, 27 March 2002; Volume 4614, pp. 28–39. [CrossRef]

30. Mbuyi-Muamba, J.M.; Dequeker, J. Biochemical anatomy of human bone: Comparative study of compact and spongy bone in femur, rib and iliac crest. *Cells Tissues Organs* **1987**, *128*, 184–187. [CrossRef]

31. Paredes, W.E.; Ari, S.F.; Geraldo, Á.B.; de Andrade, D.A. In vitro assessment of the composition and micro hardness of the hard tissues of oral cavity submitted to gamma irradiation. *Int. J. Cancer Res. Ther.* **2017**, *2*.

32. Han, P.; Ji, W.P.; Zhao, C.L.; Zhang, X.N.; Jiang, Y. Improved osteoblast proliferation, differentiation and mineralization on nanophase Ti6Al4V. *Chin. Med. J.* **2011**, *124*, 273–279. [PubMed]

33. Chou, Y.F.; Huang, W.B.; Dunn, J.C.Y.; Miller, T.A.; Wu, B.M. The effect of biomimetic apatite structure on osteoblastic activity, proliferation, and gene expression. *Biomaterials* **2005**, *26*, 285–295. [CrossRef] [PubMed]

34. Chou, L.; Marek, B.; Wagner, W.R. Effects of hydroxylapatite coating crystallinity on biosolubility, cell attachment efficiency and proliferation in vitro. *Biomaterials* **1999**, *10*, 977–985. [CrossRef]

35. Ogura, R.; Kato, H.; Okada, D.; Foxton, R.M.; Ikeda, M.; Miura, H. The relationship between bite force and oral sensation during biting in molars. *Aust. Dent. J.* **2012**, *57*, 292–299. [CrossRef] [PubMed]

36. Baker, M.I.; Eberhardt, A.W.; Martin, D.M.; McGwin, G.; Lemons, J.E. Bone properties surrounding hydroxyapatite-coated custom osseous integrated dental implants. *J. Biomed. Mater. Res. B Appl. Biomater.* **2010**, *95*, 218–224. [CrossRef] [PubMed]

37. Diez-Perez, A.; Güerri, R.; Nogues, X.; Cáceres, E.; Peña, M.J.; Mellibovsky, L. Microindentation fo in vivo measurement of bone tissue mechanical properties in humans. *J. Bone Miner. Res.* **2010**, *25*, 1877–1885. [CrossRef] [PubMed]

38. Sun, X.H.; Qiao, J.W.; Jiao, Z.M.; Wang, Z.H.; Yang, H.J.; Xu, B.S. An improved tensile deformation model for in-situ dendrite/metallic glass matrix composites. *Sci. Rep.* **2015**, *5*, 13964. [CrossRef] [PubMed]